Supporting Information for

A flexible porous Cu(II) bis-imidazolate framework with ultrahigh concentration of active sites for efficient and recyclable CO_2 capture

Dong-Dong Zhou, Chun-Ting He, Pei-Qin Liao, Wei Xue, Wei-Xiong Zhang, Hao-Long Zhou, Jie-Peng Zhang* and Xiao-Ming Chen

MOE Key Laboratory of Bioinorganic and Synthetic Chemistry, KLGHEI of Environment and Energy Chemistry, School of Chemistry & Chemical Engineering, Sun Yat-Sen University, Guangzhou 510275, P. R. China.

*E-mail: zhangjp7@mail.sysu.edu.cn

Supplementary Index

Experimental details.

Materials and General Methods. Reagents and solvents were commercially available and used without further purification. The ligand benzodiimidazole (H_2bdim) was synthesized from 1,2,4,5-benzentetramine, according to the literature procedure.[S1] IR spectra were obtained from KBr pellets on a Bruker Tensor 27 FT-IR spectrometer in the 400–4000 cm^{-1} region. Elemental analyses (C, H, N) were performed with a Vario EL elemental analyzer. Powder X-ray diffraction (PXRD) patterns were recorded using a Bruker D8 ADVANCE X-ray powder diffractometer (Cu Kα) at room temperature except otherwise stated. The composition of CO_2/N_2 gas mixture was controlled by two mass flowmeters with a total flow rate 100 mL min^{-1}. Thermogravimetry analyses were performed using a TA Q50 instrument with a heating rate of 5.0 °C/min under nitrogen. Gas sorption isotherms were measured with a Micromeritics ASAP 2020M instrument. Before the sorption experiments, the as-synthesized samples were placed in the sample tubes and dried under high vacuum at 70 ^oC for 12 h.

Synthesis. Single crystals of $[Cu_2(\mu\text{-}OH)_2(bdim)]\cdot 5.4H_2O$ (**1**) and $[Cu_2(\mu\text{-}OCH_3)_2(bdim)]\cdot C_6H_6$ (**2**). A solution of H_2bdim (1×10^{-5} mol) in MeOH (1.0 mL) was slowly and carefully layered onto a solution of $[Cu(NH_3)_2]OH$ (1×10^{-5} mol) in aqueous ammonia/methanol (1/1, 1 mL), where benzene (2 mL) was placed between the two layers. After about 4 months, dark-green crystals of **1** and **2** were obtained by manual selection.

Bulk microcrystalline powder of **1**. MeOH (20 mL) was poured into an aqueous NaOH (6 mol/L, 20 mL) solution of $Cu(OH)_2$ (0.18 g, 1.85 mmol) and stirred for several minutes to give a brownish suspension. Then a solution of H_2bdim (0.15 g, 0.95 mmol) in methanol/benzene (1/1, 40 mL) was dropwise added in 12 hrs. After the suspension was stirred for 5 days, the mixture was filtered and successively washed by H_2O and MeOH twice, then successively soaked in MeOH and H_2O for two days, and at last filtered to give the product (yield: 85%). Anal. Calcd (%) for $[Cu_2(\mu\text{-}OH)_2(bdim)]\cdot 5.4H_2O$ ($C_8H_{16.8}Cu_2N_4O_{7.4}$): C, 23.18; H, 4.08; N, 13.52. Found:

C, 23.25; H, 4.05; N, 13.42. IR (cm^{-1}, KBr): 3621(m), 3413(s, br), 1610(m), 1491(s), 1469(s), 1372(s), 1237(s), 1191(m), 1164(m), 854(m), 836(m), 639(m), 484(m), 429(m).

Crystal Structure Determination. Diffraction data of **1** and **2** were collected on a Bruker Apex and an Oxford Diffraction CCD diffractometer with graphite-monochromated Mo and Cu Kα radiation, respectively. Absorption corrections were applied by using multi-scan program SADABS and PROCESS-AUTO. The structures were solved with the direct method and refined with a full-matrix least-squares technique with the SHELXTL program package. Anisotropic thermal parameters were applied to all non-hydrogen atoms. The hydrogen atoms were generated geometrically. Crystal data as well as details of data collection and refinements for the complexes are summarized in Table S1. CCDC 956255-956256 contain the supplementary crystallographic data for this paper. These data can be obtained free of charge from The Cambridge Crystallographic Data Centre via www.ccdc.cam.ac.uk/data_request/cif.

Pawley Refinement Details. The powder X-ray diffraction data were collected with a scanning speed of 0.02 ^{o}/step and 2 sec/step. Indexing and Pawley refinement of the PXRD patterns were carried out by using the Reflex module of Material Studio 5.0. The patterns were indexed by the X-cell method with the aid of unit-cell parameters from single-crystal data. Pawley refinements were carried out with the cell parameters obtained from indexing in space group $C2/m$ and $P2_1/m$. Peak profiles, zero-shift, background, and unit-cell parameters were refined simultaneously. The peak profiles were refined by the Pseudo-Voigt function with Berar-Baldinozzi asymmetry correction parameters. The background was refined with a 20th-order polynomial.

Computational details. In this work, all the GCMC (Grand Canonical Monte Carlo) simulations were performed in the sorption modules of the Materials studio 5.0 package. Before the simulations, the model structures from the X-ray diffraction data (including both the $C2/m$ and the $P2_1/m$ lattice) were geometrically optimized by fixing the cell parameters by using the spin polarization density functional theory

(DFT) on the basis of generalized gradient approximation (GGA) with the Perdew–Burke–Ernzerhof (PBE) function. The double numerical plus polarization (DNP) basis and the DFT semi-core pseudopots (DSPP) were adopted. As the Cu(II) ion has unpaired electron, we set the multiplicity of the system as auto, and then the program would attempt to determine the ground spin state through a spin-unrestricted calculation. The atomic partial charges in the frameworks were calculated after the optimizations by using the Mulliken population analysis. However, the Mulliken charges for the Cu(II) ions were apparently too low to simulate the accurate adsorption properties of the frameworks, so we directly took the CBAC (connectivity-based atom contribution) charge for Cu, which were developed by Zhong et al.[S2]

CO_2 was also optimized using the same method (the C=O bond length is 1.177 Å) but adopted the ESP fitted charge (qO = -0.29e and qC = 0.581e). For all the GCMC simulations, the simulation box was set with 8 (2 × 2 × 2) unit cells while all the frameworks and the CO_2 molecule were considered to be rigid and described by the universal forcefield (UFF). The cutoff distance was set to 18.5 Å for the Lennard-Jones (LJ) interactions, the electrostatic interactions and the van der Waals interactions were handled using the Ewald and Atom based summation method, respectively. The favorable adsorption sites were simulated by the fixed loading task and Metropolis method at 298 K. The loading steps, equilibration steps and the production steps were all set to 1.0×10^7. The saturation/maximum uptakes were modeled at 298 K using the fixed pressure task and Metropolis method with 2.0×10^7 equilibration steps, followed by 2.0×10^7 production steps for computing the ensemble averages.

Calculation of isosteric heat of adsorption (Q_{st}).

Dual-site Langmuir−Freundlich equation[5d]

$$n = \frac{n_{\mathrm{L,A}} \times b_{\mathrm{A}} \times p^{1/t_A}}{1 + b_{\mathrm{A}} \times p^{1/t_A}} + \frac{n_{\mathrm{L,B}} \times b_{\mathrm{B}} \times p^{1/t_B}}{1 + b_{\mathrm{B}} \times p^{1/t_B}}$$

Where there are two distinct adsorption sites A and B, n is amount adsorbed, n_{L} is amount adsorbed at saturation, p is pressure, b and t are constants.

The Clausius−Clapeyron equation[S3] was employed to calculate the enthalpies of CO_2 adsorption:

$$\left[\frac{\partial \ln p}{\partial (1/T)}\right]_n = -\frac{Q_{st}}{R}$$

Where p is the pressure, n is the amount adsorbed, T is the temperature, R is the universal gas constant.

Calculation of CO_2/N_2 selectivities.[12]

Virial fitting equation

$$\ln p = \ln n + a_0 + a_1 n + a_2 n^2 + a_3 n^3 \ldots$$

where p is pressure, n is amount adsorbed, T is temperature, and a_0, a_1 etc. are Virial coefficients. a_0 is related to adsorbate–adsorbent interactions, whereas a_1 describes adsorbate–adsorbate interactions. The Henry's Law constant (K_{H}) is equal to exp(-a_0).

The Henry's Law selectivity for gas component i over j is calculated based on the following equation.

$$S_{ij} = K_{Hi} \Big/ K_{Hj}$$

Table S1. Crystallographic data and structure refinement results.

Complex	**1**	**2**
Formula	$C_8H_{16.8}Cu_2N_4O_{7.4}$	$C_{16}H_{16}Cu_2N_4O_2$
Formula weight	414.53	423.41
Temperature (K)	150(2)	128(2)
Crystal system	Monoclinic	Monoclinic
Space group	$P2_1/m$	$C2/m$
a (Å)	10.7521(8)	16.377(3)
b (Å)	11.7077(7)	12.209(2)
c (Å)	12.344(1)	10.268(2)
β (°)	92.146(7)	127.226(2)
V (Å^3)	1552.8(2)	1634.8(5)
Z	4	4
D_c (g cm^{-3})	1.773	1.720
R_1 $[I > 2\sigma(I)]^a$	0.0946	0.0385
wR_2 $[I > 2\sigma(I)]^b$	0.2790	0.0929
R_1 (all data)	0.1011	0.0552
wR_2 (all data)	0.2837	0.1009
GOF	1.046	1.028

[a] $R_1 = \sum||F_o| - |F_c||/\sum|F_o|$.

[b] $wR_2 = [\sum w(F_o^2 - F_c^2)^2/\sum w(F_o^2)^2]^{1/2}$.

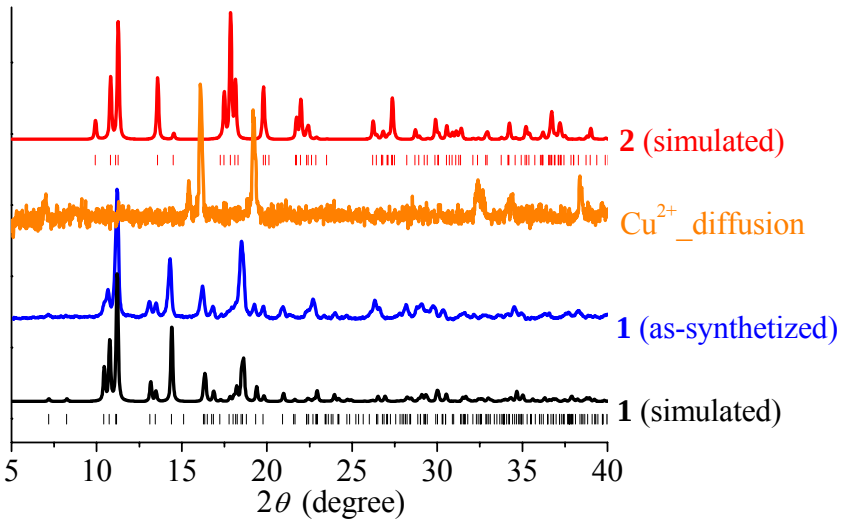

Fig. S1 PXRD patterns of solid samples obtained by different reaction methods.

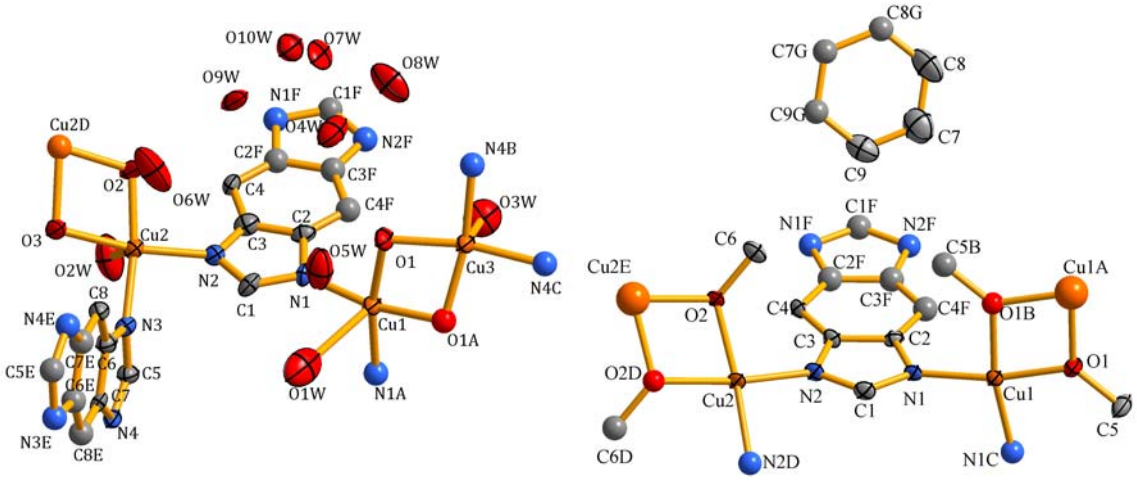

Fig. S2 The coordination environments of **1** (left, symmetric codes: A: *x*, 3/2-*y*, *z*; B: -1+*x*, *y*, *z*; C: -1+*x*, 3/2-*y*, *z*; D: *x*, 1/2-*y*, *z*; E: 2-*x*, 1-*y*, 2-*z*; F: 1-*x*, 1-*y*, 1-*z*) and **2** (right, symmetric codes: A: 1-*x*, *y*, 2-*z*; B: 1-*x*, 1-*y*, 2-*z*; C: *x*, 1-*y*, *z*; D: 1-*x*, *y*, 1-*z*; E: 1-*x*, -*y*, 1-*z*; F: 1/2-*x*, 1/2-*y*, 1-*z*; G: *x*, -*y*, *z*) (hydrogen atoms are omitted for clarity). In **1**, besides Cu1 and Cu3, O2 and O3 also lie on a mirror plane in the framework. Furthermore, a two-fold screw axis across the centre of the ligand $bdim^{2-}$. Moreover, Cu2 and O1 in **2** also lie on a two-fold axis and the centre of the ligand $bdim^{2-}$ lies across a two-fold screw axis. Cu1 and O_2 lie on a mirror plane and benzene of solvation lies across a mirror plane.

Table S2. Comparison of the key parameters of PCPs with gravimetric or volumetric CO_2 uptake similar with or higher than MAF-35. Note: the values higher than those of MAF-35 were highlighted in bold.

Compound[a] (common name)	Q_{st} (kJ/mol)	ρ (g mL^{-1})	CO_2 uptake at 298 K and 1 atm		Concentration of active sites		Type of active sites[h]	Reference
			wt %	g L^{-1}	mol kg^{-1}	mol L^{-1}		
mmen-Mg_2(dobpdc)	**71**[b]	0.750	17.0	128	5.0	3.7	OMS+LBS	5d
CAU-1	**48**[c]	0.892	17.6	157	3.7	3.3	LBS	S4
Mg_2(dobdc)	**47**[d]	0.920	**35.2**[#1]	**324**[#1]	8.2	7.6	OMS	6b
MAF-35	47[b, e]	1.357	19.6	266	12.6	17.2	OMS	This work
bio-MOF-11	45[c]	1.234	17.9	221	7.9	9.8	LBS	4g
rht-MOF-7	45[f]	0.783	17.2	135	11.2	8.8	OMS+LBS	S5
Mg_2(dobpdc)	44[b]	1.073	**22.0**	236	3.3	3.5	OMS	5d
Cu-TDPAT	42[g]	0.782	**25.9**	202	11.2	8.8	OMS+LBS	4i
Ni_2(dobdc)	41[c]	1.194	**25.6**[#1]	**306**[#1]	6.4	7.6	OMS	6b
Zn_2(ox)(atz)	41[e]	**1.713**	14.3[#2]	245[#2]	5.3	9.1	LBS	4f
Co_2(dobdc)	37[d]	1.177	**30.6**[#1]	**360**[#1]	6.4	7.6	OMS	6b
HKUST-1	35[e]	0.879	18.4	162	4.9	4.3	OMS	S6
[Cu(Me-4py-trz-ia)]	30[d]	0.928	**26.8**	249	7.7	7.1	OMS+LBS	S7
PCN-88	27[g]	0.657	18.5[#1]	122[#1]	3.3	2.2	OMS	14
MAF-66	26[g]	1.128	19.4	219	8.6	9.8	LBS	12
Cu-TPBTM	26[g]	0.627	**23.3**	146	7.0	4.4	OMS+LBS	4j

[a] mmen = N,N'-dimethylethylenediamine; BTTri = 1,3,5-tris(1H-1,2,3,-triazol-5-yl)benzene; dobpdc = 4,4'-dioxido-3,3'-biphenyldicarboxylate; dobdc = 2,5-dioxido-1,4-benzenedicarboxylate; TDPAT = 2,4,6-tris(3,5-dicarboxylphenyl-amino)-1,3,5-triazine; ox = oxalate; atz = 3-amino- 1,2,4-triazole; Me-4py-trz-ia = 5-(3-methyl-5-(pyridine-4-yl)-(4H-1,2,4-triazol-4-yl)iso- phthalate); TPBTM = N,N',N''-tris(isophthalyl)-1,3,5- benzenetricarboxamide.

[b] Obtained by the Clausius−Clapeyron equation and dual-sites Langmuir−Freundlich fitting.

[c] Obtained by the Clausius−Clapeyron equation and Langmuir−Freundlich fitting.

[d] Obtained by the Clausius−Clapeyron equation and Toth model fitting.

[e] Obtained by the Clausius−Clapeyron equation without mathematical fitting.

[f] Obtained by the Clausius−Clapeyron equation and dual-sites Langmuir fitting.

[g] Obtained by the Virial fitting method.

[#1] 296 K; [#2] 293 K.

[h] LBS = Lewis basic site.

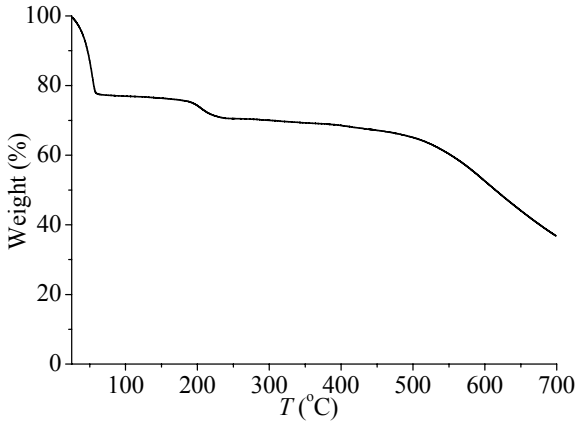

Fig. S3 Thermogravimetry curve of **1**.

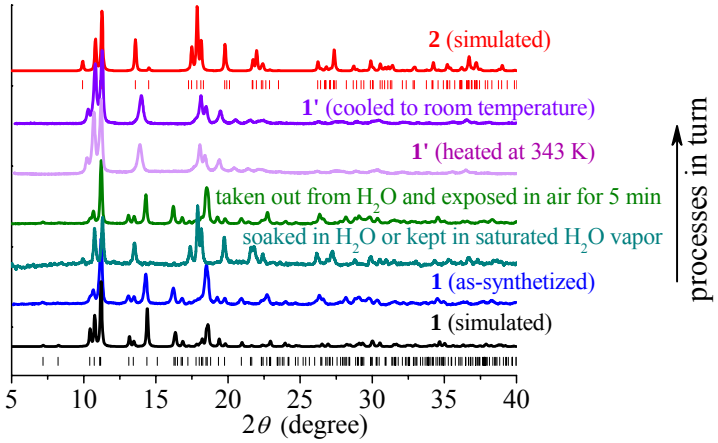

Fig. S4 PXRD patterns of **1** at different conditions.

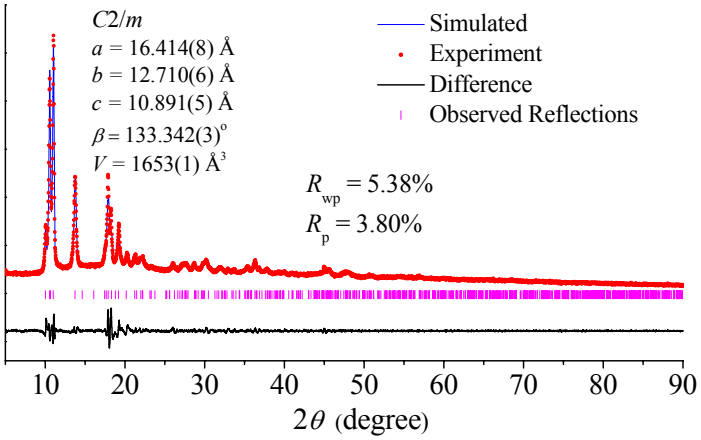

Fig. S5 Pawley refinement results of the PXRD pattern for **1'**. The obtained unit-cell parameters are similar to those of **2** [*C*2/*m*, *a* = 16.377(3) Å, *b* = 12.209(2) Å, *c* = 10.268(2) Å, β = 127.226(2)°, *V* = 1634.8(5) Å^3].

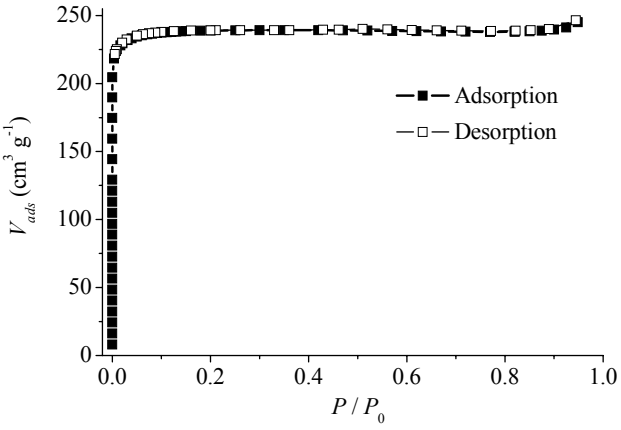

Fig. S6 N_2 sorption isotherms at 77 K.

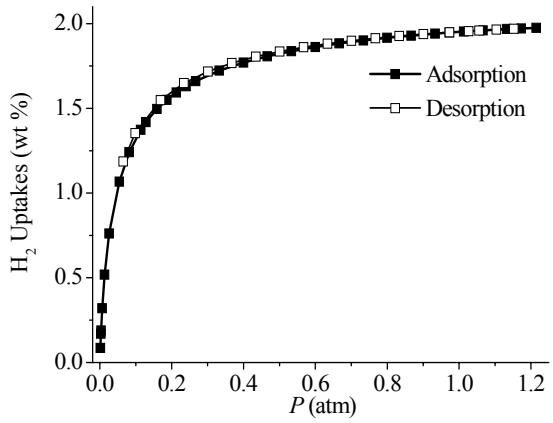

Fig. S7 H_2 sorption isotherms at 77 K.

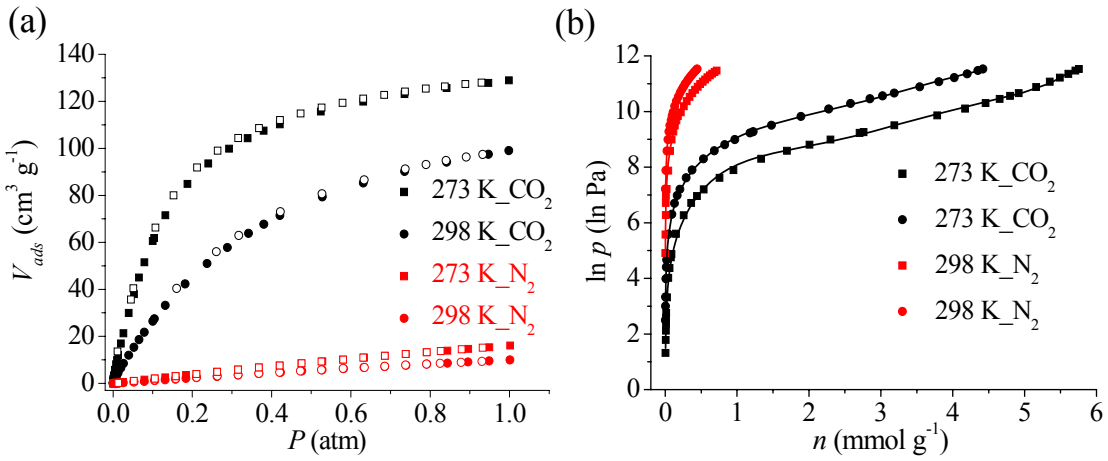

Fig. S8 (a) CO_2 and N_2 (adsorption: solid, desorption: open) isotherms measured at 273 K and 298 K, and (b) Virial fitting (lines).

Table S3. Virial fitting parameters obtained in Fig. S8b.

	CO_2		N_2	
T (K)	273	298	273	298
R^2	0.9989	0.9997	0.9963	0.9851
a_0	6.8907±0.0346	8.5322±0.0154	11.2281±0.0431	12.2930 0.0519
a_1	2.8659±0.2325	1.0260±0.0848	1.4758±0.3520	-0.0511±0.2085
a_2	-2.4713±0.3122	-0.6716±0.0975	-0.9770±0.5172	—
a_3	0.9476±0.1532	0.1991±0.0365	—	—
a_4	-0.1610±0.0310	-0.0186±0.0043	—	—
a_5	0.0102±0.0022	—	—	—

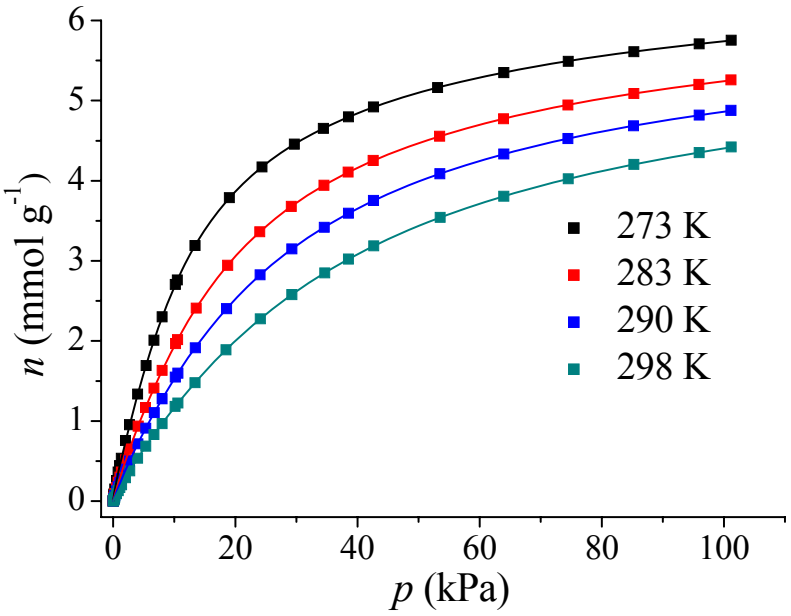

Fig. S9 Dual-site Langmuir−Freundlich fitting (lines) for CO_2 adsorption isotherm (points) measured at different temperatures.

Table S4. Langmuir−Freundlich fitting parameters obtained in Fig. S7.

T (K)	273	283	290	298
R^2	0.999999	0.999999	0.999999	0.999999
$n_{L,A}$	4.8635±0.0471	4.6857±0.0880	4.5253±0.1140	4.7064±0.1474
b_A	0.0862±0.0003	0.0592±0.0006	0.0467±0.0008	0.0330±0.0008
t_A	1.2986±0.0087	1.2161±0.0100	1.1866±0.0093	1.1302±0.0081
$n_{L,B}$	2.1420±0.0561	1.9618±0.0914	1.9008±0.1079	1.4972±0.1292
b_B	0.0194±0.0007	0.0119±0.0006	0.0081±0.0005	0.0044±0.0004
t_B	0.5932±0.0059	0.6310±0.0092	0.6485±0.0106	0.6315±0.0148

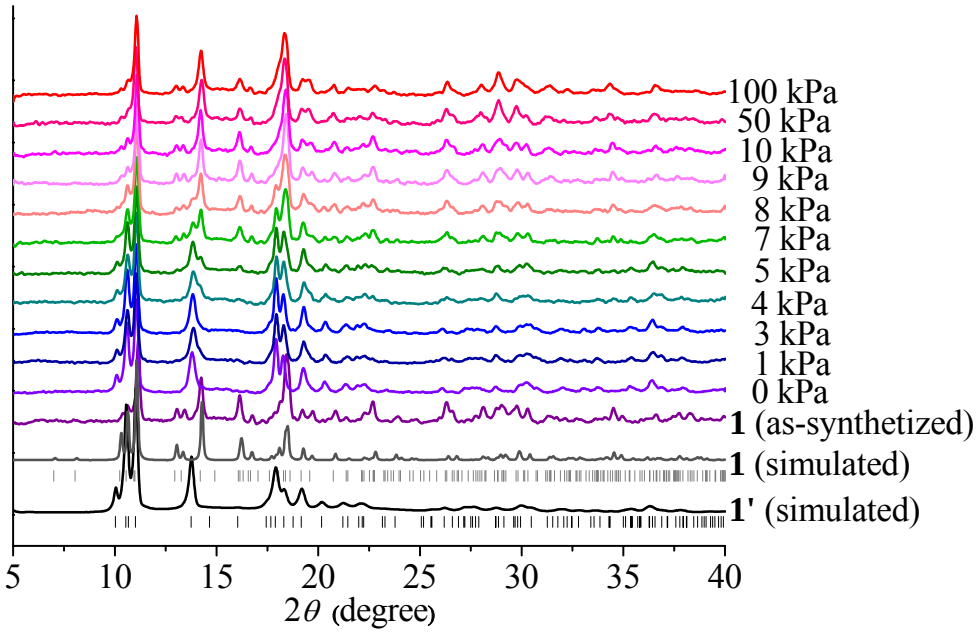

Fig. 10 PXRD patterns of **1'** at 298 K in mixed CO_2/N_2 flow with different CO_2 partial pressures.

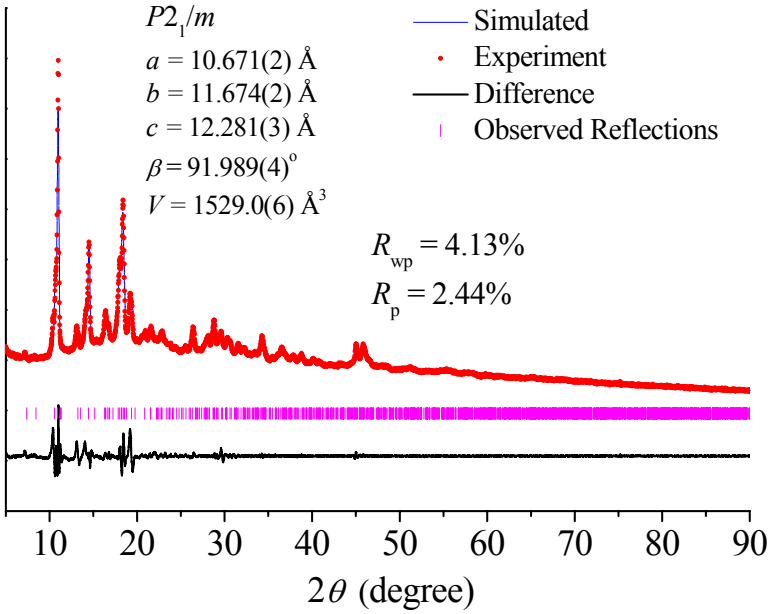

Fig. S11 Pawley refinement results of the PXRD pattern for **1'** at CO_2/N_2 (15:85, v/v). The obtained unit-cell parameters are similar to those of **1** [$P2_1/m$, a = 10.7521(8) Å, b = 11.7077(7) Å, c = 12.344(1) Å, β = 92.146(7)°, V = 1552.8(2) Å^3].

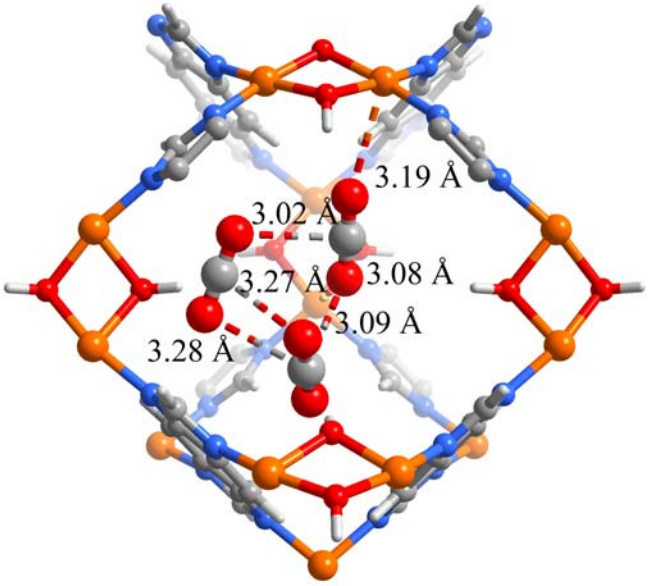

Fig. S12 GCMC simulation result of the host-guest structure of **1** at 298 K and 1 atm.

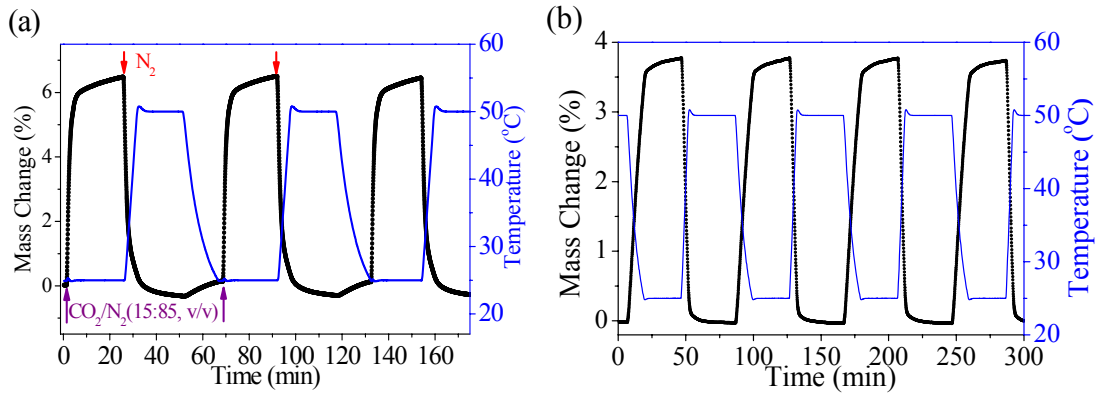

Fig. S13 (a) Repeated adsorption−desorption kinetics for **1'** under a mixed CO_2/N_2 (15:85, v/v) flow at 25 °C and a pure N_2 flow at 50 °C. (b) Temperature swing adsorption−desorption kinetics for **1'** under CO_2/N_2 (15:85, v/v) mixture gas.

References

(S1) J. Ariant, J. Marhan and H. Taeublova, *Collect. Czech. Chem. Commun.,* 1960, **25**, 1602.

(S2) Q. Xu and C. Zhong, *J. Phys. Chem. C,* 2010, **114**, 5035.

(S3) L. Czepirski and J. Jagiello, *Chem. Eng. Sci.,* 1989, **44**, 797.

(S4) X. Si, C. Jiao, F. Li, J. Zhang, S. Wang, S. Liu, Z. Li, L. Sun, F. Xu, Z. Gabelica and C. Schick, *Energy Environ. Sci.,* 2011, **4**, 4522.

(S5) R. Luebke, J. F. Eubank, A. J. Cairns, Y. Belmabkhout, L. Wojtas and M. Eddaoudi, *Chem. Commun.,* 2012, **48**, 1455.

(S6) Q. Min Wang, D. Shen, M. Bülow, M. Ling Lau, S. Deng, F. R. Fitch, N. O. Lemcoff and J. Semanscin, *Microporous and Mesoporous Mater.,* 2002, **55**, 217.

(S7) D. Lassig, J. Lincke, J. Moellmer, C. Reichenbach, A. Moeller, R. Glaser, G. Kalies, K. A. Cychosz, M. Thommes, R. Staudt and H. Krautscheid, *Angew. Chem., Int. Ed.,* 2011, **50**, 10344.